# A Numerical Study of the Impact of Bending and Torsional Stiffness on the Static Aeroelastic Characteristics of a Large Aspect Ratio Composite Wing

Shengjun Qiao*, Fei Wang and Keping Wang

School of Aircraft Engineering, Xi'an Aeronautical Institute, Xi'an, 710077, China


**INFORMATION**

**Keywords:**
Numerical calculation
high aspect ratio
bending and torsional stiffness
static elasticity
lift-drag ratio
deflection

**DOI:** 10.23967/j.rimni.2024.10.56530

SCIPEDIA Revista Internacional de Métodos Numéricos para Cálculo y Diseño en Ingeniería

RIMNI Revista Internacional Métodos numéricos para cálculo y diseño en ingeniería

# A Numerical Study of the Impact of Bending and Torsional Stiffness on the Static Aeroelastic Characteristics of a Large Aspect Ratio Composite Wing

**Shengjun Qiao*, Fei Wang and Keping Wang**

School of Aircraft Engineering, Xi'an Aeronautical Institute, Xi'an, 710077, China

**ABSTRACT**

The bending and torsional stiffness influence structural deformation to varying degrees. Utilizing the coupled numerical method of Computational Fluid Dynamics and Computational Structural Dynamics (CFD/CSD), a comprehensive study was conducted on the impact of bending and torsional stiffness on the static aeroelastic behavior of a high-aspect-ratio wing, employing FLUENT software across diverse flight conditions. The study summarized this influence by comparing the computational outcomes. The results indicate that as the angle of attack rises, the lift increment diminishes gradually until the angle reaches 14 degrees, rendering the strategy of enhancing bending and torsional stiffness to gain more lift ineffective. Between 2 and 14 degrees of angle of attack, the lift difference between the scenarios decreases from 23.98% to 7.31%. At higher Mach numbers and lower angles of attack, augmenting wing stiffness significantly boosts wing lift. Optimal lift-to-drag characteristics are achieved at approximately 6 degrees of angle of attack. By averagely increasing the wing's bending and torsional stiffness by 8.28% and 5.22%, respectively, the lift-to-drag characteristics can be enhanced by 5.27% at a low angle of attack of 0.75 Mach. The disparity in maximum deflection between the two stiffness wings is most pronounced at higher flight speeds and smaller angles of attack, with the opposite trend observed for the difference in maximum torsion angle. The key findings presented in this paper can expedite the integrated design of stiffness for this type of wing structure by providing vital technical insights.

**OPEN ACCESS**

**Received:** 24/07/2024

**Accepted:** 22/10/2024

**DOI**
10.23967/j.rimni.2024.10.56530

**Keywords:**
Numerical calculation
high aspect ratio
bending and torsional stiffness
static elasticity
lift-drag ratio
deflection

## 1 Introduction

The high aspect ratio wing will produce large bending and torsional deformation under the action of airflow, which will seriously affect the flight performance and flight safety of the airplane, and the key factor that determines the large deformation of this wing is the stiffness characteristics of the wing structure. Therefore, the effect of stiffness needs to be taken into account in the design of wings with high aspect ratios. A large number of analyses and experimental results carried out on two-dimensional wings and three-dimensional wings show that the bending and torsional stiffnesses of high aspect ratio wings have a great influence on the static aeroelasticity and flutter characteristics of the wings.

*Correspondence: Shengjun Qiao (qiaoshengjun123@163.com). 

In terms of static aeroelastic analysis, in recent years, researchers from many universities and research institutes at home and abroad have done a lot of research work on static aeroelastic analysis methods for wings with high aspect ratios, and most of them are based on the CFD/CSD coupling method to carry out static aeroelastic analysis considering the structural geometrical nonlinearities, and the results show that the effects of structural geometrical nonlinearities must be considered in carrying out the static aeroelastic analysis of wings with high aspect ratios [1–4]. Bouma et al. [5] investigated the effect of structural and aerodynamic nonlinearities on an aeroelastic system with three degrees of freedom, and the results of the comparative study showed that the unsteady-state representation of the aerodynamic loads is essential for the correct prediction of the flutter speed, the type of instability, and the dynamics of the system, even with small reductions in the frequency and small angles of attack.

In terms of the effect of stiffness on static aeroelasticity, Mao et al. [6] took a 15-m wingspan solar aircraft as a research object and modified the stiffness of the main beams of the wing according to the target flutter speed, so as to realize the inverse modeling of the dynamics of the solar aircraft and perform flutter analysis based on it. Wang et al. [7] took a wind blade airfoil as a research object and put forward an integrated aerodynamic performance of the airfoil and the structural stiffness characteristics of the airfoil. Chen et al. [8] took the large spreading ratio wing as the research object, established a full elastic aerodynamic inverse evaluation model with wing stiffness as the independent variable, and carried out the sensitivity analysis of wing stiffness based on the fluid-structure coupling method. The results of the study show that the vertical bending stiffness and twist stiffness are the main characteristics that affect the wing twist angle and lift. And linear relationship between elastic aerodynamic derivatives and stiffness ratio is established. Based on the fluid-solid coupling method, the structural calculation adopts their own introduced higher-order structural calculation model, and the fluid calculation adopts the open-source software SU2, and the static aeroelasticity analysis is carried out on composite wings, and the proposed calculation method is verified [9]. Hao et al. [10] applied the static aeroelasticity calculation method based on the fluid-solid coupling to the “Ionwind”, which is a new type of airfoil. Hao et al. [10] applied the method based on fluid-structure coupling to the “ionic wind” propulsion systems, and carried out the static aeroelastic analysis, and investigated the effect of the stiffness characteristics of the system on the static aeroelasticity. Tsushima et al. [11] utilized the Co-structure coupling method on the composite wing and validated the suggested calculation approach. They also employed the Co-rotational method for the nonlinear static aeroelastic analysis of a composite/corrugated wing.

In terms of additive manufacturing, Zhu et al. [12] took a high aspect ratio aircraft as the object of study, considering the need to carry out wind tunnel tests, however, the stiffness of the traditional shrinkage model is insufficient, a feasible static aeroelastic analytical model of additively fabricated integrated shells for improving the stiffness of the wing is developed based on the additive manufacturing technology. Tsushima et al. [13] developed a geometrical nonlinear aeroelastic analytical model and validated it experimentally and verified the accuracy of additive manufacturing and its feasibility for wind tunnel testing.

There are fewer research works at home and abroad on the effect of stiffness on aerodynamic elasticity of wings, and more comprehensive optimization designs containing stiffness are carried out, considering that stiffness is closely related to aerodynamic elasticity of airplanes. In order to meet the aeroelasticity requirements more effectively during the structural design process, the thesis continues to study the effect of bending and torsional stiffness characteristics on static aeroelasticity based on the geometrically nonlinear static aeroelasticity analysis method, stiffness calculation method, and fluid-structure coupling analysis method that have been carried out by our team before. The research

results can provide an important reference for those who are engaged in the stiffness design of such wing structures.

## 2 Methods of Wing Bending and Torsional Stiffness and Static Aeroelastic Analysis

Based on our previous research on the stiffness characteristics of a high aspect ratio composite wing, we summarized that [14], the geometrical parameters of the wing beams, which are the main load-bearing structures of the wing, have a large influence on the wing profile stiffness, especially the bending and torsional stiffness, and the dimensions of the wing beams have a particularly serious influence on the wing stiffness characteristics in terms of the dimensions of the main load-bearing structures and the rms sensitivity of the layouts. Changing the geometrical parameters of the beams, the bending and torsional stiffnesses of the wing sections undergo relatively large changes in the three-beam wing section where the rudder is located, resulting in a deviation of the stiffness center position. In order to study the influence of the bending and torsional stiffness on the static aeroelasticity, the influence of the bending and torsional stiffness on the wing pressure distribution, lift-drag characteristics and deformation is investigated by increasing the geometric parameters of the beams, which will provide theoretical support for the design of this type of wing stiffness and the details of the static aeroelasticity.

The geometric parameters of the beams and stringers are shown in Tables 1 and 2, respectively. The cross-sectional shape of the stringer is shown in Fig. 1. The wing cross-sectional shape and main bearing structure layout are shown in Fig. 2. The material parameters after equivalence are shown in Table 3. The size distribution of the geometrical parameters of the beams on the wings is uneven, and the geometrical parameters of the three parts of the beams are increased by 16.7%, 25%, and 25%, respectively, and the bending and torsional stiffness distributions of the two wings along the spreading direction of the profiles obtained are shown in Figs. 3 and 4, respectively [15]. The bending and torsional stiffness distributions of the wing along the spanwise sections are not uniform when the geometrical parameters of the beams are increased by the same percentage, but all of them show large changes in the wing section where the ailerons are located. The torsional stiffness increments ranged between $7.71 \times 10^5 \sim 1.72 \times 10^8$ N·m/rad, while the bending stiffness increments ranged between $2.15 \times 10^7 \sim 1.07 \times 10^8$ N/m.

**Table 1:** Thicknesses of the spar webs/mm

| Model | Section A |
|---|---|
| Original | 3 |
| Enlarged | 3.5 |

**Table 2:** Stringer dimensions/mm

| Models | Upper surface of the wing | | | | Lower surface of the wing | | | |
|---|---|---|---|---|---|---|---|---|
| | W | H | t | W1 | W | H | t | W1 |
| Original | 40 | 30 | 3 | 25 | 30 | 30 | 3 | 25 |
| Enlarge | 45 | 35 | 3.5 | 30 | 25 | 25 | 3.5 | 30 |

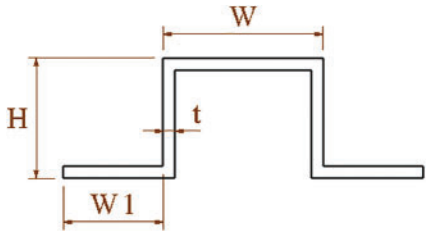


**Figure 1:** Stringer cross-section

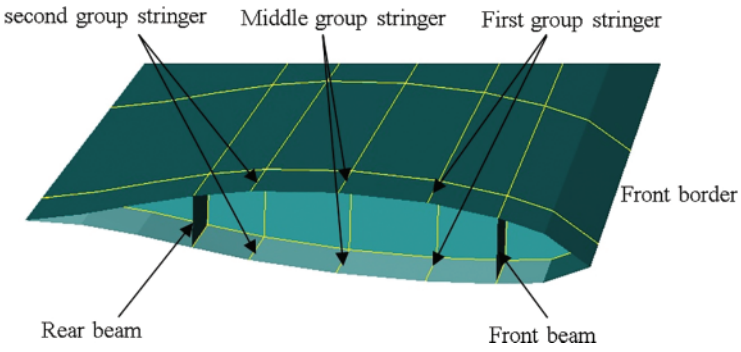


**Figure 2:** Wing cross sections

**Table 3:** Material parameters

| Structures | Parameters after equivalence/MPa |
|---|---|
| Spar web | E = 57100, G = 16200, v = 0.491 |
| Stringer | E = 57100, G = 16200, v = 0.491 |
| Skin | E = 61100, G = 15300, v = 0.487 |

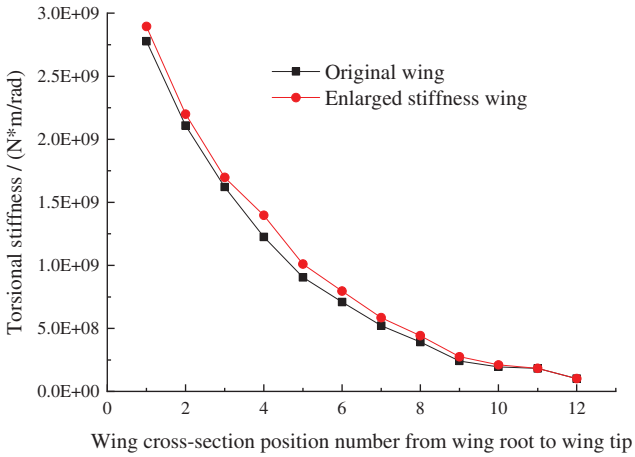


**Figure 3:** Torsional stiffness distribution of the two wings

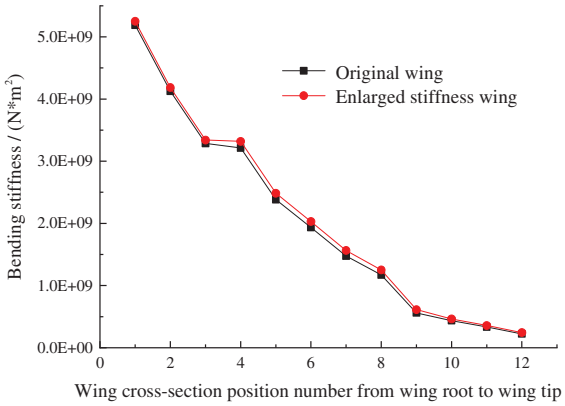


**Figure 4:** Bending stiffness distribution of the two wings

The structural computational theory during the static aeroelastic analysis is based on the Co-rotational (CR)-based structural geometric nonlinear method developed by our team in 2018 as shown in literature [1], which will not be repeated here. The main flow of the coupled CFD/CSD-based analysis is shown in Fig. 5.

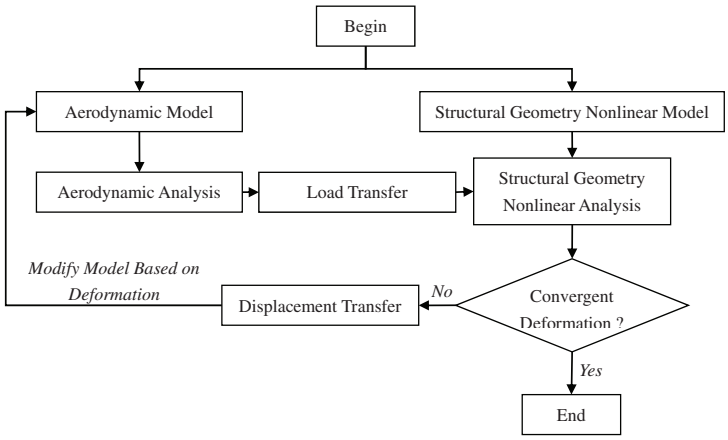


**Figure 5:** Analysis process of static aeroelasticity

The load and displacement information transfer techniques [1] that we use during the static aeroelastic analysis are as follows:

**(1) Load information interpolation method**

First, we extract the pressure on the surface of the wing from the calculation results of the FLUENT software. In the manner, the pressure values of the computational fluid dynamic (CFD) node on the coupling surface in the $x$, $y$ and $z$ directions can be obtained.

$$\begin{Bmatrix} G_x \\ G_y \\ G_z \end{Bmatrix} = S \cdot P \cdot \begin{Bmatrix} n_x \\ n_y \\ n_z \end{Bmatrix} \tag{1}$$

where $G_x$, $G_y$, and $G_z$ represent the pressure in three directions, $S$ is the area of influence of pressure $P$, and $n_x$, $n_y$, and $n_z$ represent the three unit vertical vectors of CFD.

The pressure information interpolation method is used to identify the structural grid adjacent to each CFD node. When performing the pressure information conversion, the CFD node must be within the computational structure dynamics (CSD) element, and the distance between the CFD and the CSD nodes must be minimized. Finally, the nodal loads for the structural analysis are obtained.

$$\mathrm{F} = \sum_{i=1}^{n} F_i^{'} \tag{2}$$

where $F_i^{'}$ is the load transferred from each CFD node to the structural node, which can be expressed as

$$\begin{bmatrix} F_{x,i} \\ F_{y,i} \\ F_{z,i} \end{bmatrix} = \begin{bmatrix} A_i/A & 0 & 0 \\ 0 & A_i/A & 0 \\ 0 & 0 & A_i/A \end{bmatrix} \tag{3}$$

where $F_{x,i}$, $F_{y,i}$, and $F_{z,i}$ are the loads used for the structural calculations, $A_i$ is the triangular area composed of one CFD node and two CSD nodes, and $A$ is the triangular area composed of three CSD nodes.

**(2) Displacement information interpolation method**

To choose an ideal data transfer method, we must consider a variety of factors. Based on the constant volume transformation (CVT) method [16], the parameter of the minimum area is introduced, and finally, an enhanced CVT method is established. This method exhibits a high computational efficiency and is easy to program. The following text describes the main steps of using the enhanced CVT method to perform the displacement information conversion.

The elements close to each node $\overline{\alpha}(t)$ in the aerodynamic model must be identified. These nodes are replaced by $\overline{S_i}(t)$, $\overline{S_j}(t)$, and $\overline{S_k}(t)$. As time elapses, the relationship can be expressed as follows:

$$\overline{\alpha}(t) = \alpha\overline{S_i}(t) + \beta\overline{S_j}(t) + \gamma\overline{S_k}(t) + v(t)\left[\left(\overline{S_j}(t) - \overline{S_i}(t)\right) \times \left(\overline{S_k}(t) - \overline{S_i}(t)\right)\right] \tag{4}$$

where $\alpha$, $\beta$, and $\gamma$ are constants and satisfy the formula $\alpha + \beta = \gamma$; "$\times$" represents the vector product. The selection of values of $\alpha$, $\beta$, and $\gamma$ must satisfy the initial conditions, expressed in Eq. (5).

$$\overline{\alpha}^{p}(0) = \alpha\overline{S_i}(0) + \beta\overline{S_j}(0) + \gamma\overline{S_k}(0) \tag{5}$$

$\overline{\alpha}^{p}(0)$ represents the orthogonal projection. By substituting $\alpha$, $\beta$, and $\gamma$ into Eq. (4), we can obtain the value of $v(0)$.

$$\overline{\alpha}(0) = \alpha\overline{S_i}(0) + \beta\overline{S_j}(0) + \gamma\overline{S_k}(0) + v(0)\left[\left(\overline{S_j}(0) - \overline{S_i}(0)\right) \times \left(\overline{S_k}(0) - \overline{S_i}(0)\right)\right] \tag{6}$$

The node information pertaining to the aerodynamic model after time $t$ can be obtained using Eq. (6). In the determination of $v(t)$, the law of conservation of volume must be satisfied. The tetrahedron is composed of a node in the aerodynamic model and three structural nodes, leading to a total of four noncoplanar nodes.

The model with high aspect ratio wing (HARW) is shown in Fig. 6. The whole computation zone for aerodynamic analysis is shown in Fig. 7. The wing half-span is 7.595 m, and the sweep angle is 9°. The skin on the wing, beams and stringers are laminated composite structure, the wing part of the control surface is a three-beam structure, and the rest is a double-beam structure; the wing trailing edge is arranged with two control surfaces. The whole computation zone containing 167,948 nodes and 957,832 elements is made of unstructured and tetrahedral elements for aerodynamic analysis. The dimensions of the domain of the HARW are 100 m × 60 m × 60 m.

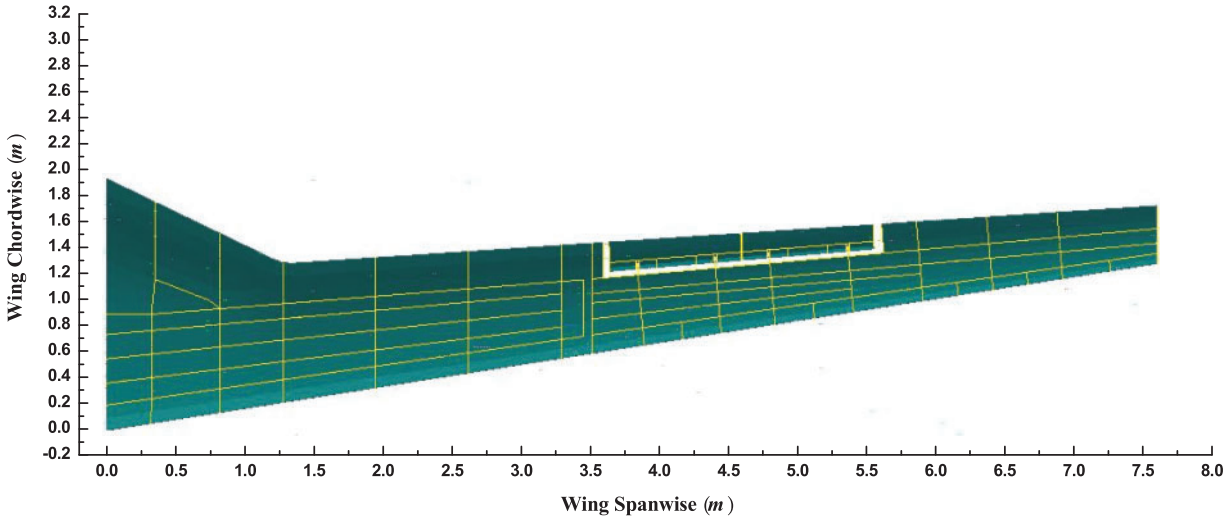


**Figure 6:** Wing finite element model

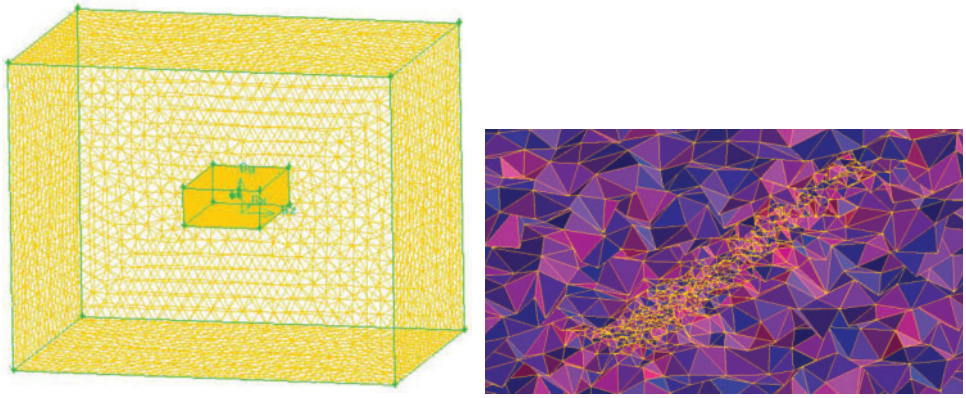

(a) (b)

**Figure 7:** Whole computation zone and local tetrahedral mesh (a) Whole computation zone; (b) Local tetrahedral mesh map of the coupling surface

## 3 Degree of Influence of Bending and Torsional Stiffness on Airfoil Pressure Distribution

For wings with high aspect ratios, the amount of force on the skin under airflow depends directly on the main internal bearing structure of the wing that is connected to the skin. Therefore, the size of the geometric parameters of the beam, as the main bearing structure of this type of airfoil, seriously affects the pressure magnitude and its distribution on the airfoil surface. It is necessary to carry out a study on the effect of the geometrical parameters of the beam, i.e., the cross sectional stiffness of the wing, on its pressure distribution. In this paper, the nonlinear static aeroelastic analyses are carried out at a flight speed of 0.56 and 0.75 Ma, and an angle of attack ranging from 2° to 14° at a flight altitude of 13 km for a composite wing with different stiffness distributions, respectively. The pressure distributions of the upper and lower wings at 13.1%, 40.8% and 83.6% of the profiles (2x/b) for the two types of wings with original stiffness and enlarged stiffness are shown in Figs. 8 to 11, respectively.

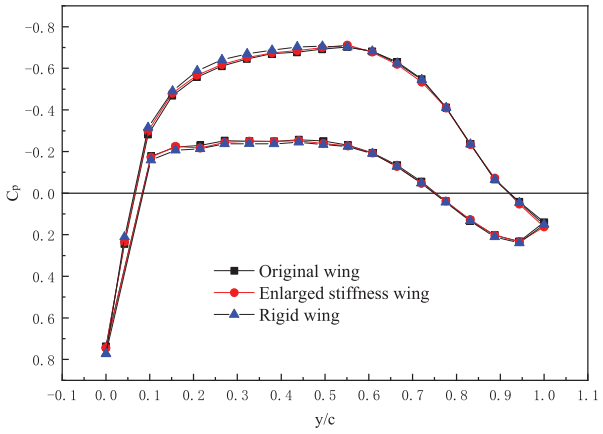


(a)

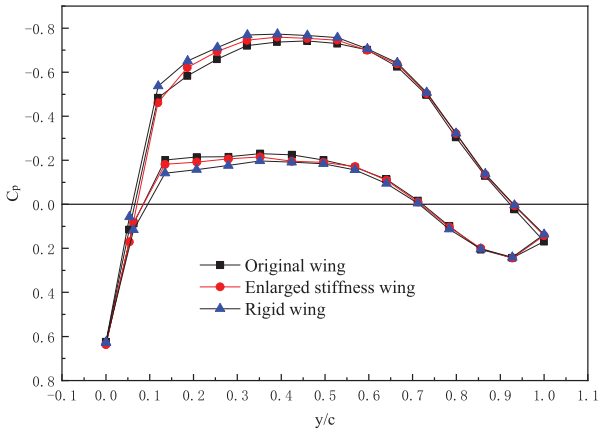


(b)

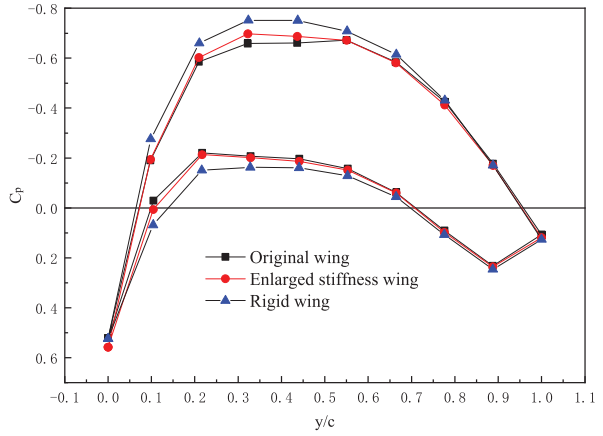


(c)

**Figure 8:** Pressure at 0.56 Ma (a = 2°) (a) 2x/b = 13.1%; (b) 2x/b = 40.8%; (c) 2x/b = 83.6%

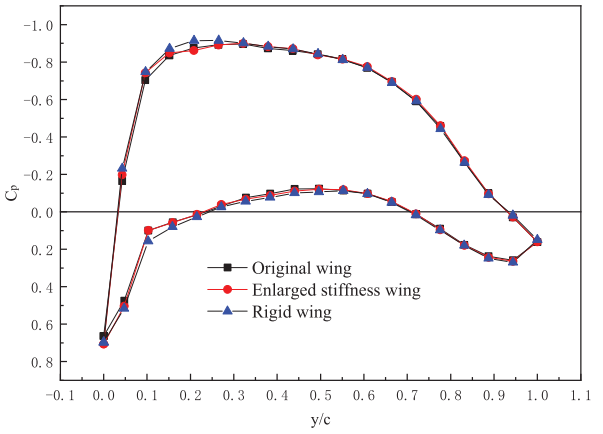


(a)

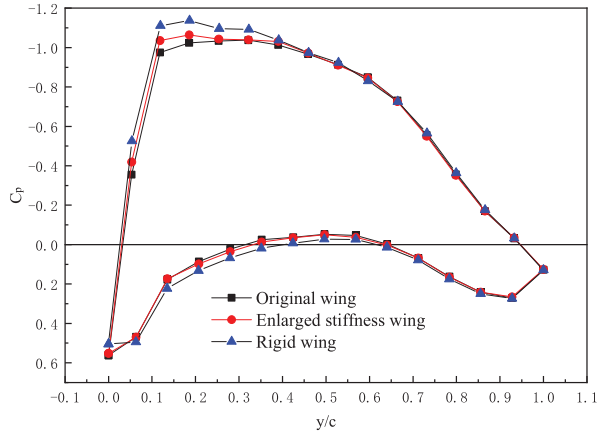


(b)

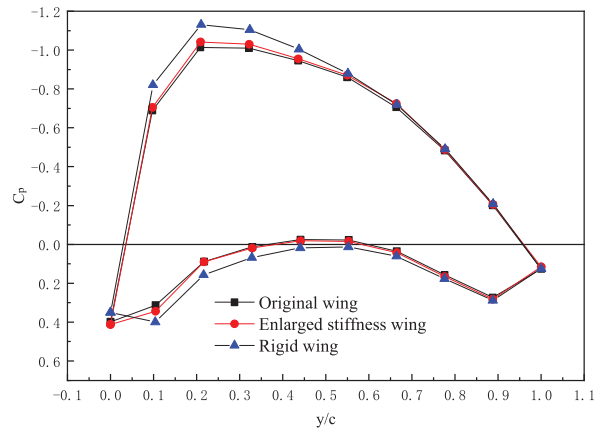


(c)

**Figure 9:** Pressure at 0.56 Ma (a = 6°) (a) 2x/b = 13.1%; (b) 2x/b = 40.8%; (c) 2x/b = 83.6%

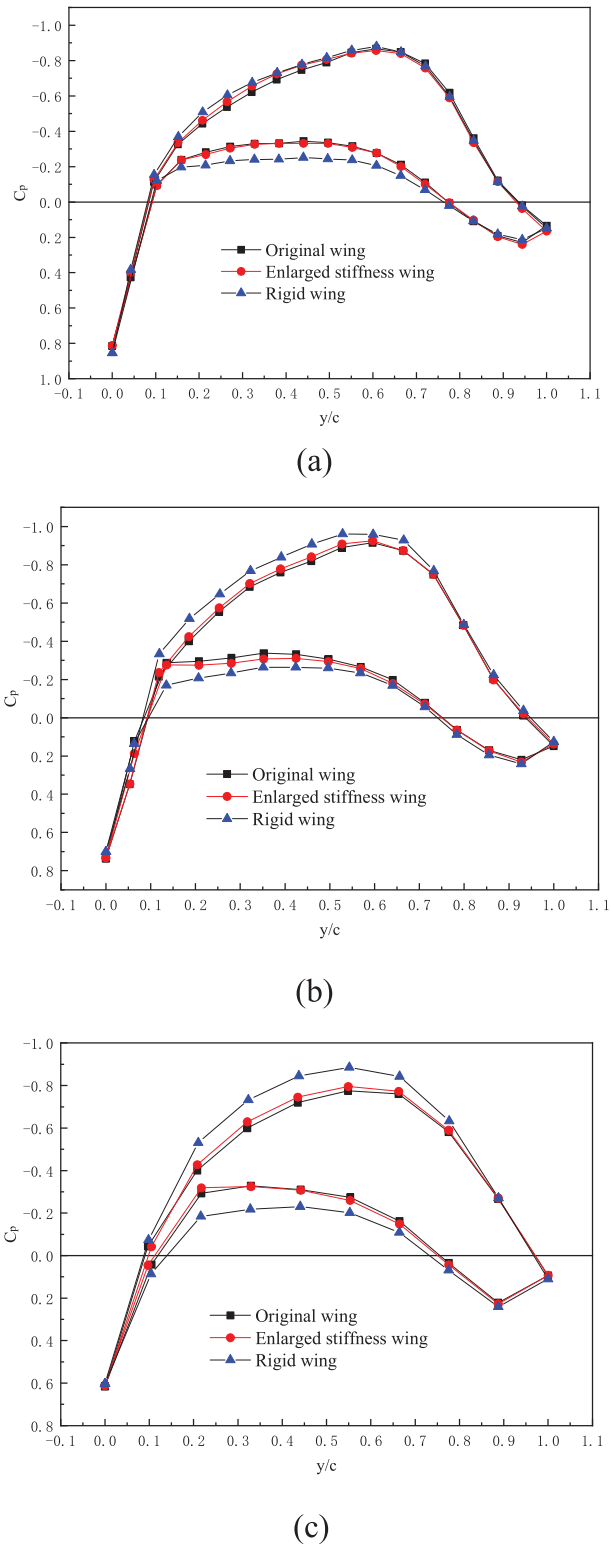


**Figure 10:** Pressure at 0.75 Ma (a = 2°) (a) 2x/b = 13.1%; (b) 2x/b = 40.8%; (c) 2x/b = 83.6%

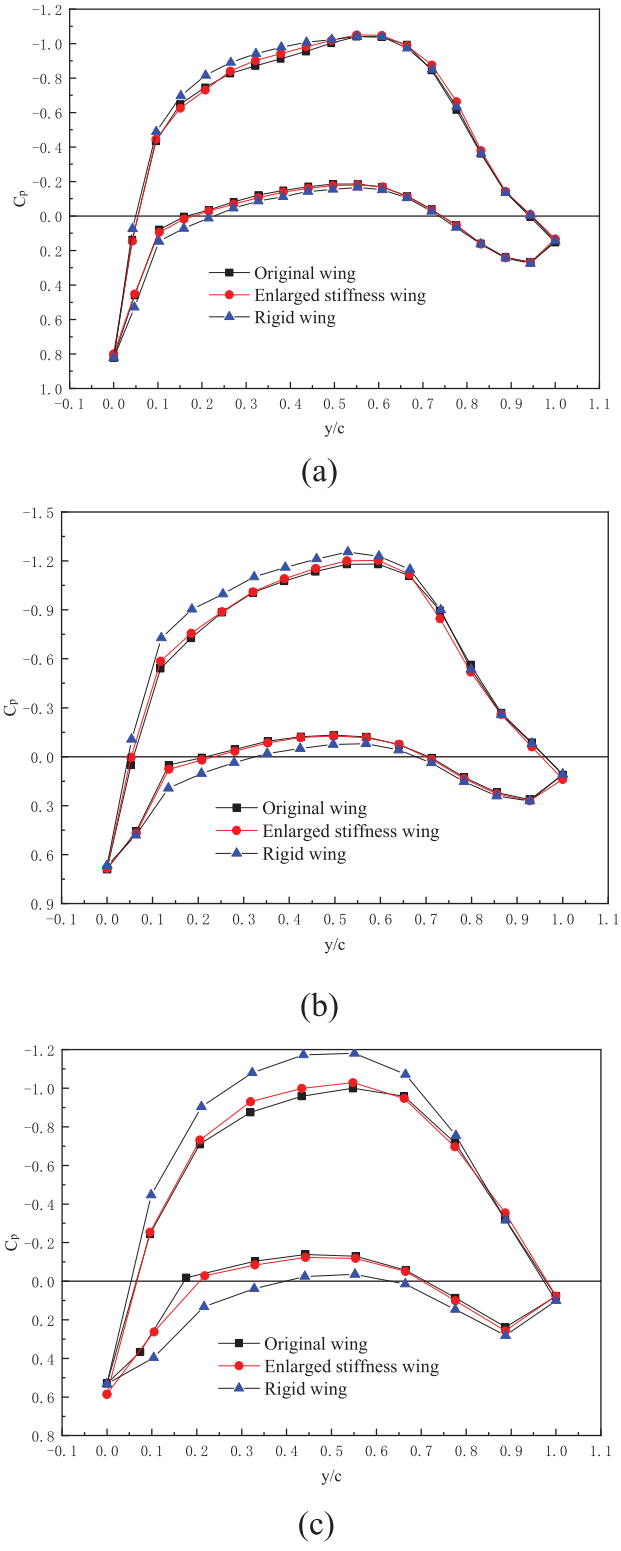


**Figure 11:** Pressure at 0.75 Ma (a = 6°) (a) 2x/b = 13.1%; (b) 2x/b = 40.8%; (c) 2x/b = 83.6%

From Figs. 8 and 9, it can be seen that the elastic deformation of the inner wing segments of the two wings is small, and its effect on the aerodynamic loads is also small. The outer wing segment has a larger deformation, and the pressure changes more and more obviously with the increase of deformation. Due to the combined effect of bending and torsional stiffness, the relative changes in pressure at the bottom and the top of the high aspect ratio flexible wing are different. In contrast, the pressure changes are relatively large at locations with large deformations. Increasing the stiffness reduces the elastic deformation, which makes the pressure distribution on the surface of the wing tend to the tip direction and increases the bending moment at the root of the wing. Increasing the angle of attack makes the pressure distribution tends to the fuselage direction again, reducing the bending moment relative to the fuselage. When the wing tip deflection is less than 12% of the half-span length, the influence of the stiffness on the aerodynamic loads of the wing is weak, so the bending stiffness has a large design space. In the structural design, it is necessary to appropriately reduce the wing bending and torsional stiffness and appropriately increase the leveling angle of attack, so as to achieve the purpose of improving the surface pressure distribution of the wing structure.

It can also be seen from Figs. 10 and 11 that the effects of bending and torsional stiffness on the pressure distribution of the wing are relatively obvious when the flight speed is increased under the condition that the leveling angle of attack remains unchanged. The wing surface pressure distribution tends to change more and more obviously in the direction of the wing tip, but the effect of stiffness is still mainly reflected in the wing section between the front and rear beams.

The maximum pressure difference between the two wings under the two flight speed conditions occurs in the upper and lower airfoil surfaces between the front and rear beams under different angles of attack, and the pressure coefficient difference between the upper and lower surfaces of the two wings increases with the increase of the leveling angle of attack. The upper airfoil load is obviously smaller than the lower airfoil load, the upper airfoil is in suction state, and both wings show that the leading edge load is larger than the trailing edge load. Under the flight speed of 0.56 Ma, both pressure differences are small, and the maximum pressure difference between the upper and lower surfaces occurs near the front beam. When the flight speed increases to 0.75 Ma, the pressure difference between the upper and lower surfaces of both wings between the front and rear beams increases slightly, and the maximum pressure difference between the upper and lower surfaces occurs between the front and rear beams near the rear beam. Compared with the effect of stiffness on the angle of attack, flight speed becomes the main factor.

Under constant conditions, the different stiffness levels have varying degrees of impact on surface pressure, albeit minor. Stiffness has an insignificant effect on pressure distribution at positions closer to the wing root ($2x/b = 13.1\%$). However, as flight speed and angle of attack increase, stiffness has a certain influence on pressure distribution at positions further from the wing root ($2x/b = 40.8\%$ and $2x/b = 83.6\%$). Increasing stiffness slightly enhances the pressure difference on the wing surface. In general, stiffness has a minor impact on the pressure distribution on the upper and lower surfaces of high aspect ratio composite wings, especially at lower angles of attack and flight speeds. Aerodynamic shape becomes the most direct factor influencing pressure distribution on the upper and lower wing surfaces. In the aeroelastic design process of such wings, when the wingtip displacement exceeds 12% of the half-span length, the influence of stiffness should be considered for a comprehensive design of stiffness and aerodynamic elasticity for the wing.

## 4 The Impact of Bending and Torsional Stiffness on Lift-Drag Characteristics

Aircraft lift and drag characteristics are typically presented in terms of lift coefficient, drag coefficient, and their increments, which depend on the aircraft's configuration and flight conditions. Stiffness not only affects the pressure distribution on the wings but also influences the redistribution of aerodynamic loads and changes in lift. The curves showing the variation of lift with angle of attack under conditions of speeds at 0.56 and 0.75 Ma and angle of attack ranging from 2 to 14 degrees are depicted in Figs. 12 and 13, respectively.

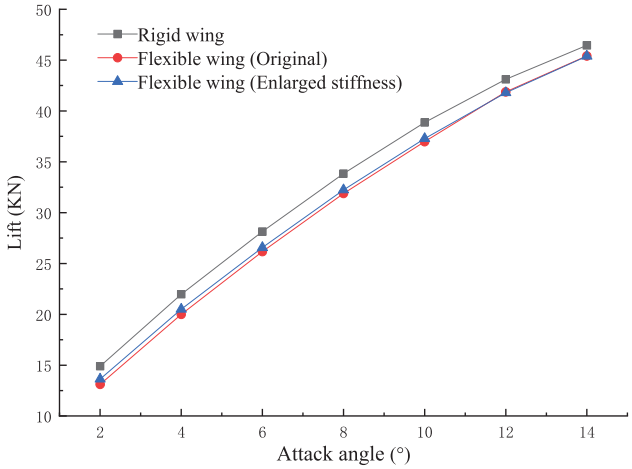


**Figure 12:** The lift curve with angle of attack for wings of different bending and torsional stiffness (0.56 Ma)

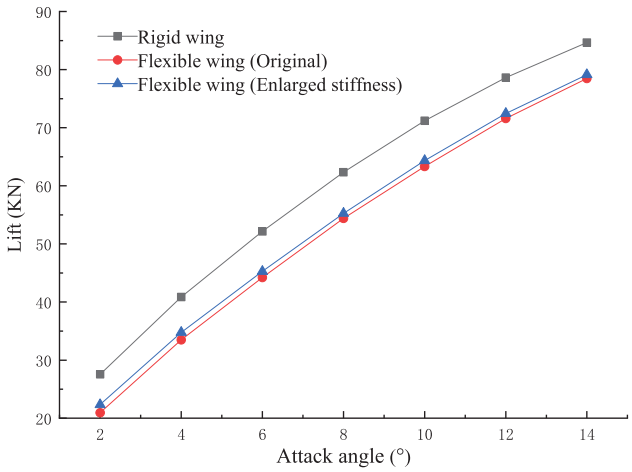


**Figure 13:** The lift curve with angle of attack for wings of different bending and torsional stiffness (0.75 Ma)

The lift of the two types of wings, one with enlarged stiffness and the other with original stiffness, increases as the angle of attack increases, with a gradually decreasing rate of increase. Increasing the stiffness further enhances the lift of the wings. At a flight speed of 0.56 Ma, the increase in lift is relatively small, whereas at a speed of 0.75 Ma, the increase in lift is significant.

Increasing the stiffness of the wings can enhance lift at different angles of attack, but the degree of lift enhancement varies noticeably. As the angle of attack increases, the lift gained by increasing the torsional stiffness decreases. When the torsional stiffness of the wings is increased by an average of 8.28% and 5.22%, respectively, the proportion of lift increase at a speed of 0.75 Ma and an angle of 2 degrees reaches 6.68%. As the angle of attack continues to increase, the rate of lift increase gradually decreases, until at an angle of attack of 14 degrees, the method of further increasing lift by increasing torsional stiffness is no longer effective. Under the same flight speed conditions, as the angle of attack increases, the lift obtained by elastic wings gradually approaches that of rigid wings. At a flight speed of 0.56 Ma, as the angle of attack increases from 2 to 14 degrees, the difference in lift between them decreases from 11.97% to 2.25%. At a flight speed of 0.75 Ma, as the angle of attack increases from 2 degrees to 14 degrees, the difference in lift between them decreases from 23.98% to 7.31%.

Increasing the wing's torsional stiffness for different speeds and angles of attack can improve the lift caused by structural deformation. For two wings with different stiffness, the change in lift is not significant at lower Mach numbers and higher angles of attack. Conversely, at higher Mach numbers and lower angles of attack, increasing the wing stiffness can significantly enhance the wing lift. Within a certain range of angles of attack, the larger the angle of attack, the closer the lift obtained by the elastic wing is to that obtained by the rigid wing.

Under the conditions of two different flight speeds ranging from 0.56 to 0.75 Ma and angles of attack varying from 2 to 14 degrees, the drag curves with respect to the angle of attack obtained are shown in Fig. 14 and 15. For the two flight speed conditions mentioned above, the drag of both the original stiffness and enlarged stiffness wings increases with the increase in trim angle, with a slightly larger magnitude of increase. The increase in stiffness not only enhances the lift of the wing but also causes an increase in drag, with a smaller increment in drag at a Mach number of 0.56 Ma. As the Mach number increases to 0.75 Ma, the increment in drag slightly increases, with a slightly larger magnitude of improvement. For different flight speeds within the range of 2 to 14 degrees of attack angle, the maximum proportion by which increasing stiffness increases the wing drag is only 2.27%.

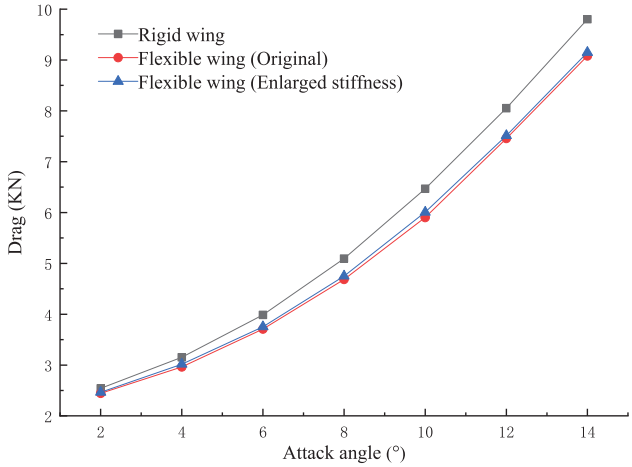


**Figure 14:** The drag curve with angle of attack for wings of different bending and torsional stiffness (0.56 Ma)

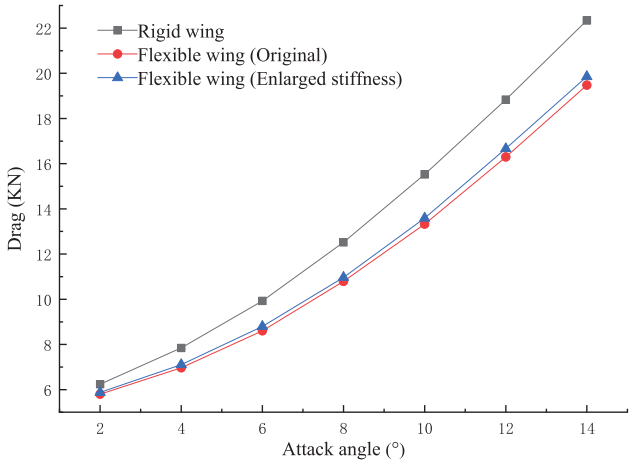


**Figure 15:** The drag curve with angle of attack for wings of different bending and torsional stiffness (0.75 Ma)

There are significant differences in the rate of change of lift and drag as the angle of attack is increased. To further determine the extent to which the angle of attack affects the lift-drag ratio of the wing under different bending and torsional stiffness conditions, we conducted a comprehensive analysis of the lift-drag characteristics. The lift-drag ratios obtained vary with the angle of attack as shown in Figs. 16 and 17. Under the same angle of attack conditions, the lift-drag ratios of wings with original stiffness and enlarged stiffness are much greater at a flight speed of 0.56 Ma than at 0.75 Ma. The lift-drag ratios of wings with different bending and torsional stiffness increase and then decrease with increasing angle of attack at both flight speeds, but the magnitude of the change is noticeably different.

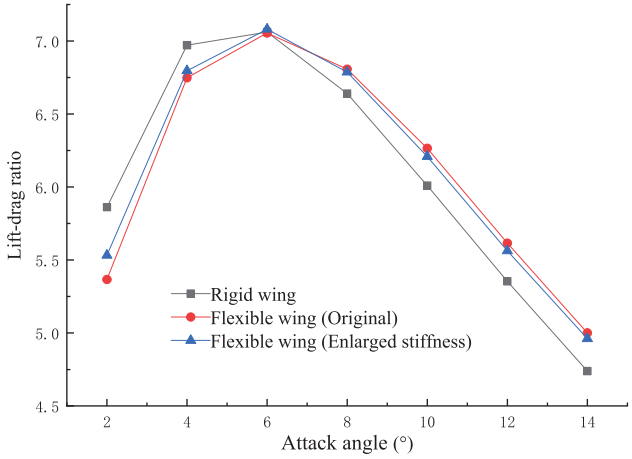


**Figure 16:** The lift-drag ratio curve with angle of attack for wings of different bending and torsional stiffness (0.56 Ma)

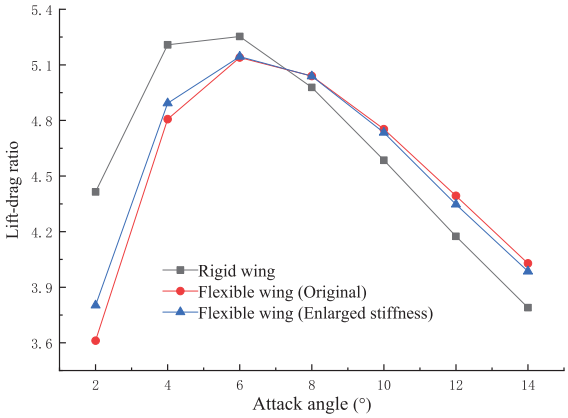


**Figure 17:** The lift-drag ratio curve with angle of attack for wings of different bending and torsional stiffness (0.75 Ma)

Under these two speed conditions, the lift-drag ratio of wings with different stiffness reaches its maximum at a 6-degree angle of attack, with minimal difference. Increasing the wing bending and torsional stiffness improves the lift-drag characteristics at angles of attack less than 6 degrees. However, when the angle of attack exceeds 6 degrees, increasing the wing bending and torsional stiffness decreases the lift-drag characteristics. With an average increase in wing bending and torsional stiffness of 8.28% and 5.22%, respectively, under the 0.56 Ma condition, the lift-drag characteristics of the wing can be improved by 3.09% at small angles of attack, while under the 0.75 Ma condition, the lift-drag characteristics of the wing can be improved by 5.27% at small angles of attack.

## 5 Effect of Bending and Torsional Stiffness on Static Aeroelastic Deformation

The objective of this study is to conduct nonlinear static aeroelastic analysis under different flight conditions for wings with original stiffness and enlarged stiffness. The distribution of profile deflection and torsional deformation of elastic wings under various flight conditions will also be studied. Performing nonlinear static aeroelastic analysis at 2° and 6° trim angles, 0.56 and 0.75 Ma flight speeds, and at an altitude of 13 km, obtaining the variation curves of profile deflection and torsional deformation of the two elastic wings at 0.56 and 0.75 Ma flight speeds with respect to angle of attack as shown in Figs. 18 and 19, respectively.

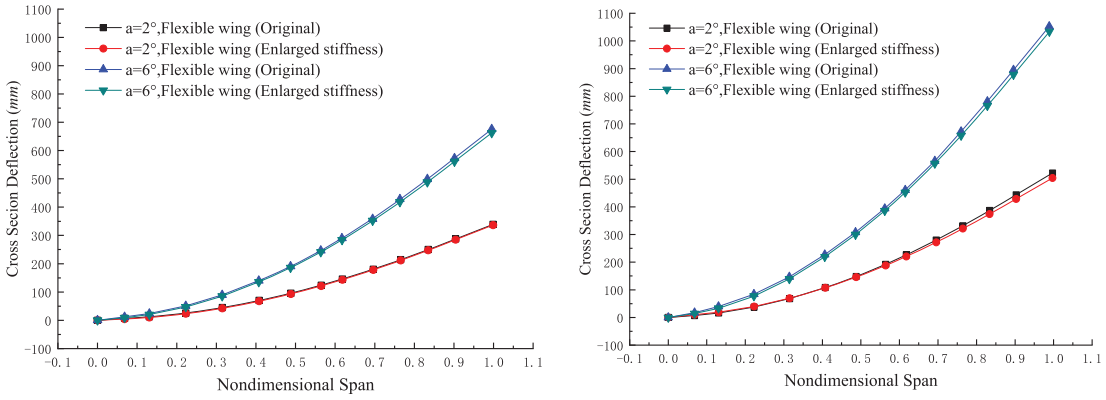


**Figure 18:** The curve of the wing cross section deflection with attack angle (a) 0.56 Ma; (b) 0.75 Ma

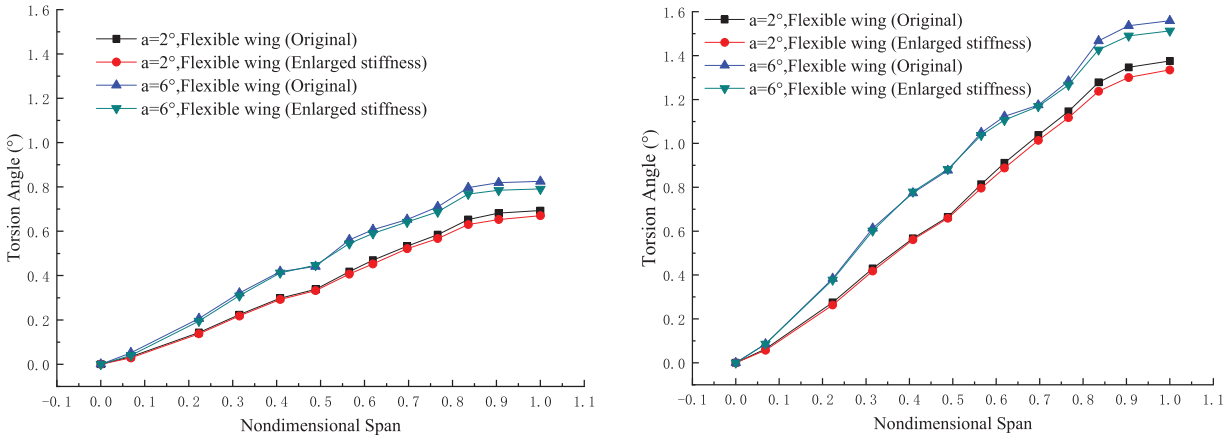


**Figure 19:** The curve of the torsion angle of the wing cross section with the attack angle (a) 0.56 Ma; (b) 0.75 Ma

Under two flight speed conditions of 0.56 and 0.75 Ma, the difference in deflection between the original stiffness and enlarged stiffness wing profiles increases. The maximum displacement of the original stiffness wing is slightly greater than that of the enlarged stiffness wing. Both wings exhibit a similar trend of twist deformation along the spanwise cross-section, but the stiffness has a relatively larger impact on the twist deformation of the wing cross-section. The twist deformations both slow down at 50% and 83% of the span length, mainly due to changes in the number of beams in the wing structure at these locations, transitioning from double beams to triple beams at 50% and from triple beams to double beams at 83%.

The comparison of the maximum deflection and torsion values of the two types of wings are shown in Tables 4 and 5. Further exploration of the impact of stiffness on the static aeroelastic deformation of the wings will be discussed with specific numerical values. The maximum deformation of the two types of wings with original stiffness and enlarged stiffness, as well as their difference, are obtained under four flight conditions in Tables 4 and 5.

**Table 4:** Deflection of the wing under different conditions

| Flight speed (Ma) | Angle of attack (°) | Maximum deflection of the original stiffness wing (mm) | Maximum deflection of the enlarged stiffness wing (mm) | Deflection reduction (%) |
|---|---|---|---|---|
| 0.56 | a = 2 | 339.115 | 336.318 | 0.83 |
| 0.56 | a = 6 | 675.478 | 662.341 | 1.95 |
| 0.75 | a = 2 | 522.490 | 504.24 | 3.5 |
| 0.75 | a = 6 | 1052.244 | 1033.392 | 1.8 |

**Table 5:** Torsional deformation of wings under different conditions

| Flight speed (Ma) | Angle of attack (°) | Maximum torsional deformation of the original stiffness wing (°) | Maximum torsional deformation of the enlarged stiffness wing (°) | Torsional deformation reduction (%) |
|---|---|---|---|---|
| 0.56 | a = 2 | 0.693 | 0.671 | 3.18 |
| 0.56 | a = 6 | 0.825 | 0.791 | 4.12 |
| 0.75 | a = 2 | 1.376 | 1.335 | 2.98 |
| 0.75 | a = 6 | 1.559 | 1.513 | 1.8 |

The values in both Tables 4 and 5 clearly show that stiffness has the ability to resist deformation, and the wing with higher stiffness has relatively less deformation. The difference in maximum deflection between the two stiffnesses is maximized at higher flight speeds and smaller angles of attack, while the difference in maximum torsional deformation between the two stiffnesses is maximized at lower flight speeds and larger angles of attack. Overall, the effect of stiffness on the torsional deformation of this high aspect ratio wing is slightly larger than that of deflection.

## 6 Conclusions

The paper carries out a study on the degree of influence of bending and torsional stiffness on the pressure distribution, lift-drag characteristics and deformation of wings with high aspect ratios under different flight speeds and various angles of attack. The conclusions are as follows:

1) For different speeds and angles of attack, increasing the bending and torsional stiffness of the wing can serve to improve the lift caused by structural deformation. The change in wing lift is not significant at lower Mach number and higher angle of attack conditions. On the contrary, at higher Mach numbers and lower angles of attack, increasing the wing stiffness can significantly improve the wing lift. Within a certain range of angle of attack, the larger the angle of attack is, the closer the lift obtained by an elastic wing is to that obtained by a rigid wing.
2) Different stiffness of the wing, always in a small angle of attack range to achieve the most lift-drag ratio. The higher the flight speed, the more the lift-drag characteristics of the wing increase at small angles of attack.
3) At higher flight speeds and smaller angles of attack, the difference in maximum deflection of wings with different stiffnesses reaches a maximum, while at lower flight speeds and larger angles of attack, the difference in maximum twist angle of wings with different stiffnesses reaches a maximum. Overall, the effect of stiffness on the torsion of the wing with high aspect ratio is slightly larger than that of deflection.
4) In the process of the aeroelastic design of this type of wing, when the wing tip displacement is greater than 12% of the half-span length, then it is necessary to consider the effect of stiffness, and carry out the integrated design of stiffness and aeroelasticity for the wing.

**Acknowledgement:** None.

**Funding Statement:** This research was funded by the Natural Science Basic Research Plan in Shaanxi Province of China, grant number is 2023-JC-YB-076.

**Author Contributions:** The authors confirm contribution to the paper as follows: study conception and design: Shengjun Qiao; data collection: Fei Wang, Keping Wang; analysis and interpretation of results: Shengjun Qiao, Fei Wang, Keping Wang; draft manuscript preparation: Shengjun Qiao, Fei Wang. All authors reviewed the results and approved the final version of the manuscript.

**Availability of Data and Materials:** The datasets generated and/or analyzed during the current study are available from the corresponding author on reasonable request.

**Ethics Approval:** The research for the paper does not involve humans or animals.

**Conflicts of Interest:** The authors declare no conflicts of interest to report regarding the present study.

## References

1. Qiao SJ, Gao HS, Lyu Y, Hua L, Wang FS. Nonlinear aeroelastic characteristics analysis of composite wing with high aspect ratio based on co-rotational method. J Fluid Struct. 2018;82(1):619–37. doi:10.1016/j.jfluidstructs.2018.07.009.
2. Reza K, Hossein S, Hassan H. Nonlinear aeroelastic analysis of a composite wing by finite element method. Compos Struct. 2014;113(4):118–26. doi:10.1016/j.compstruct.2014.03.012.
3. Nie XY, Huang CD, Yang GW. Numerical analysis for aeroelastic with structural geometrical nonlinearity using a CFD/CSD-coupled method. J Vib Shock. 2016;35(8):48–53 (In Chinese).
4. Zhang BS, Wang JL, Liu ZY, Li JY, Feng YR. Research on geometric nonlinear static aeroelasticity of high-aspect-ratio composite wing. Compos Sci Eng. 2023;2023(4):78–86 (In Chinese).
5. Bouma A, Vasconcellos R, Abdelkefi A. Nonlinear aeroelastic modeling and comparative studies of three degree of freedom wing-based systems. Int J Non Linear Mech. 2023;149(6):1–18. doi:10.1016/j.ijnonlinmec.2022.104326.
6. Mao YQ, Yang F, Gu YS. Research on flutter characteristics and stiffness design for 15 meters span wing of a solar powered aircraft. Adv Aero Sci Eng. 2019;10(4):536–41 (In Chinese).
7. Wang Q, Chen XT, Hu MJ, Zeng LL. Optimization design of wind turbine wings based on aerodynamic performance and stiffness characteristics. China Mech Eng. 2020;31(19):2283–9 (In Chinese). doi:10.3969/j.issn.1004-132X.2020.19.003.
8. Chen K, Liu XY, Cheng P, Mao K. Research on the static aero-elastic sensitivity of stiffness of flexible wing. J Exp Fluid Mech. 2022;36(6):54–60 (In Chinese).
9. Grifò M, Ronch Da A, Benedetti I. A computational aeroelastic framework based on high-order structural models and high-fidelity aerodynamics. Aerosp Sci Technol. 2023;132(1275):1–18. doi:10.1016/j.ast.2022.108069.
10. Hao S, Ma TL, Chen S, Ma HZ, Xiang JW, Ouyang FX. Static aeroelasticity of the propulsion system of ion propulsion unmanned aerial vehicles. Propulsion Power Res. 2023;12(3):1–20. doi:10.1016/j.jppr.2023.01.001.
11. Tsushima N, Yokozeki T, Su WH, Arizono H. Geometrically nonlinear static aeroelastic analysis of composite morphing wing with corrugated structures. Aerosp Sci Technol. 2019;88:244–57. doi:10.1016/j.ast.2019.03.025.
12. Zhu WJ, Miao K, Li DC. Static aeroelastic models with integrated stiffness-contributing shell structures built by additive manufacturing. Eng Struct. 2019;187:352–61. doi:10.1016/j.engstruct.2019.02.066.

13. Tsushima N, Tamayama M, Arizono H, Makihara K. Geometrically nonlinear aeroelastic characteristics of highly flexible wing fabricated by additive manufacturing. Aerosp Sci Technol. 2021;117:1–9. doi:10.1016/j.ast.2021.106923.
14. Qiao SJ, Ma RX, Jiao J, Ma XT, Liu X. The impact and sensitivity analysis of beam and stringer for stiffness center of composite wing structure. Rev Int Métodos Numér Cálc Diseño Ing. 2021;37(3):1–12. doi:10.23967/j.rimni.2021.09.009.
15. Qiao SJ, Jiao J, Ni YG, Chen H, Liu X. Effect of stiffness on flutter of composite wings with high aspect ratio. Math Probl Eng. 2021;2021(4):6683032. doi:10.1155/2021/6683032.
16. Xu M, Chen SL. Study of date exchange method for coupling computational CFD/CSD. Chin J Appl Mech. 2004;21:33–6 (In Chinese).